

HT2009-88032

PERFORMANCE ANALYSIS FOR MECHANICAL DRAFT COOLING TOWER

Si Y. LeeSavannah River National Laboratory
si.lee@srnl.doe.gov
803-725-8462**Alfred J. Garrett**Savannah River National Laboratory
alfred.garrett@srnl.doe.gov
803-725-4870**James S. Bollinger**Savannah River National Laboratory
james02.bollinger@srnl.doe.gov
803-725-1417**Larry D. Koffman**Savannah River National Laboratory
larry.koffman@srnl.doe.gov
803-725-1038**ABSTRACT**

Industrial processes use mechanical draft cooling towers (MDCT's) to dissipate waste heat by transferring heat from water to air via evaporative cooling, which causes air humidification. The Savannah River Site (SRS) has cross-flow and counter-current MDCT's consisting of four independent compartments called cells. Each cell has its own fan to help maximize heat transfer between ambient air and circulated water. The primary objective of the work is to simulate the cooling tower performance for the counter-current cooling tower and to conduct a parametric study under different fan speeds and ambient air conditions.

The Savannah River National Laboratory (SRNL) developed a computational fluid dynamics (CFD) model and performed the benchmarking analysis against the integral measurement results to accomplish the objective. The model uses three-dimensional steady-state momentum, continuity equations, air-vapor species balance equation, and two-equation turbulence as the basic governing equations. It was assumed that vapor phase is always transported by the continuous air phase with no slip velocity. In this case, water droplet component was considered as discrete phase for the interfacial heat and mass transfer via Lagrangian approach. Thus, the air-vapor mixture model with discrete water droplet phase is used for the analysis.

A series of parametric calculations was performed to investigate the impact of wind speeds and ambient conditions on the thermal performance of the cooling tower when fans were operating and when they were turned off. The model was also benchmarked against the literature data and the SRS integral test results for key parameters such as air temperature

and humidity at the tower exit and water temperature for given ambient conditions. Detailed results will be published here.

Keywords: Cooling Tower, Computational Fluid Dynamics, Heat Transfer, Mechanical Draft Cooling Tower

INTRODUCTION

Mechanical draft cooling towers are designed to cool process water via sensible and latent heat transfer to air. Heat and mass transfer take place simultaneously. Heat is transferred as sensible heat due to the temperature difference between liquid and gas phases, and as the latent heat of the water as it evaporates. Mass of water vapor is transferred due to the difference between the vapor pressure at the air-liquid interface and the partial pressure of water vapor in the bulk of the air. Equations to govern these phenomena are discussed here. The governing equations are solved by taking a computational fluid dynamics (CFD) approach.

The purpose of the work is to develop a three-dimensional CFD model to evaluate the flow patterns inside the cooling cell driven by cooling fan and wind, considering the cooling fans to be on or off. A cooling tower considered here is mechanical draft cooling tower (MDCT) consisting of four compartment cells as shown in Fig. 1. It is 9.25m wide, 31.19m long, and 9.1m high. Each cell has its own cooling fan and shroud without any flow communications between two adjacent cells except for 9-inch gap above the free surface of the water collection basin. There is an array of spray nozzles through which water droplet falls down into the cell region of the fill region cooled by the ambient air driven by fan and wind, and it is eventually collected in basin area. It is basically a counter-current MDCT at SRS. As shown in Fig. 1, about 0.15-m thick drift eliminator allows ambient air to be humidified through the

This paper has been authored by Savannah River Nuclear Solutions, LLC under Contract No. DE-AC09-08SR22470 with the U. S. Department of Energy. The United States Government retains, and by accepting the article for publication, the publisher acknowledges that the United States Government retains, a non-exclusive, paid-up, irrevocable, worldwide license to publish or reproduce the published form of this work, or allow others to do so, for United States Government purposes.

evaporative cooling process without entrainment of water droplets into the shroud exit.

This paper will focus on the thermal performance analysis for the counter-current cooling tower at SRS. The analysis of the cross-flow cooling tower is provided in the previous work [1].

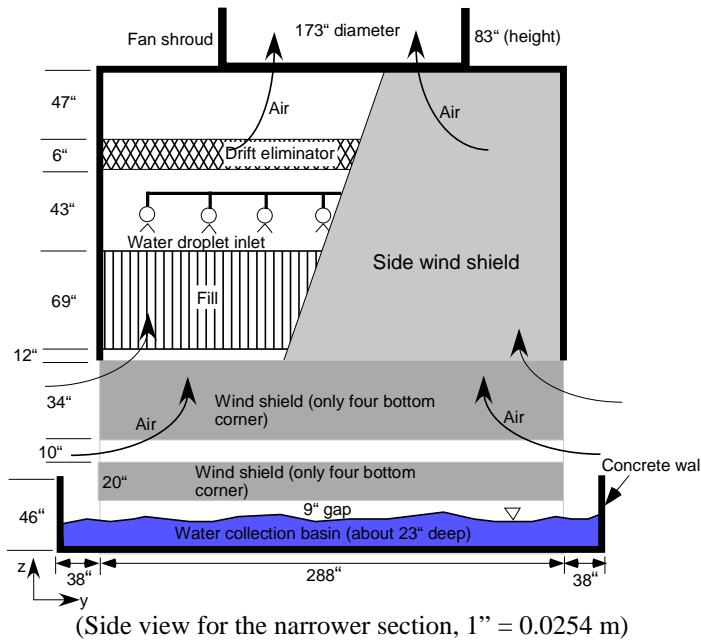
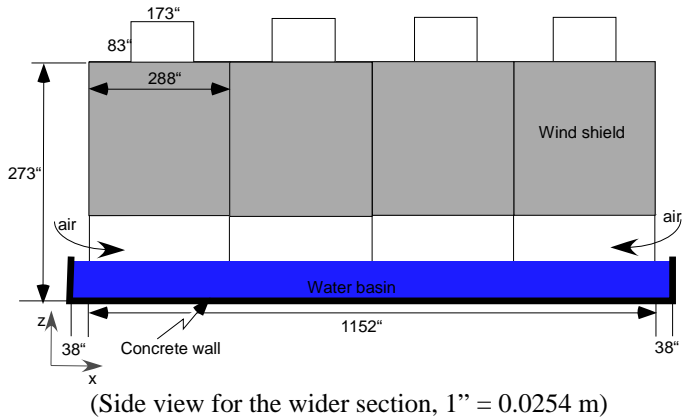


Fig. 1. Geometry and dimensions for each of the four cells in Mechanical Draft Cooling Tower (MDCT)

NOMENCLATURE

°C	Degree Centigrade (or Celsius)
CFD	Computational Fluid Dynamics
DOE	U.S. Department of Energy
d_p	Droplet diameter
hr	Hour

kg	Kilogram
m	Meter
m_w	Total water flowrate (kg/sec)
mm	millimeter
min	Minute
MDCT	Mechanical Draft Cooling Tower
PN	Plant north
TN	True north
Re	Reynolds number ($\rho u \mu$)
RH	Relative humidity
RSM	Reynolds Stress Model
s or sec	Second
SRNL	Savannah River National Laboratory
T_{amb}	Ambient air temperature (°C)
T_{wi}	Water temperature at water distribution deck (°C)
u_{ex}	Air velocity at exit of fan shroud (m/sec)
U_o	Wind speed (m/sec)
x, y, z	Three coordinate system for the computational domain as shown Fig. 1
γ_{amb}	Vapor mass fraction at ambient condition
γ_{exit}	Vapor mass fraction at cell exit
θ_o	Wind direction w.r.t. plant north
κ	Turbulence kinetic energy (m^2/sec^2)
ε	Turbulence dissipation rate (m^2/sec^3)
μ	Dynamic viscosity (kg/m-sec)
η	Nondimensional air exit velocity
ζ	Nondimensional wind direction

MODELING APPROACH AND SOLUTION METHOD

The present work took a three-dimensional CFD approach. The modeling domain was parallelepiped, and it was about 8 times larger than the actual size of the four-cell MDCT in Fig. 1 to calculate the air flow patterns inside and outside the tower cells. Cooling fan of each cell was modeled as momentum source at the shroud region since air velocity at shroud exit was continuously measured. The air-vapor mixture model was considered, assuming that vapor phase is always transported by the continuous air phase with no slip. In this situation, water droplet component was considered as discrete phase for the interfacial heat and mass transfer to air via Lagrangian approach. The droplet temperature is updated along the particle trajectory according to a heat balance, assuming the radiative cooling effect to be negligible inside the cooling tower cell. The force balance for each droplet equates the particle inertia with forces acting on a spherical particle of uniform size, d_p . In this work, water distributions at the water spray inlet are assumed to be uniform for computational efficiency. Thus, the air-vapor mixture model coupled with discrete water droplet phase is used for the analysis.

The governing equations to be solved for the modeling domain are one air-vapor mixture balance, one vapor species transport, three momentum conservations along x -, y -, and z -coordinate systems for the modeling domain, two standard turbulence equations, and one air-vapor mixture energy

balance. $\kappa\text{-}\epsilon$ standard turbulent model is used for simulation of the turbulent airflow. The solution method is presented in Fig. 2.

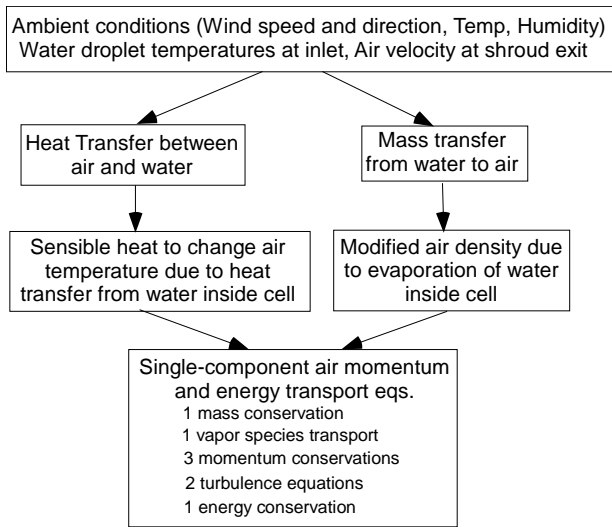


Fig. 2. Solution methods for single-phase mixture modeling approach.

TEST DESCRIPTIONS AND MODEL VALIDATION

Experimental Measurement

The compartment cells of the four-cell countercurrent-flow MDCT at SRS was instrumented at the exit of shroud region and near the water collection basin. Sensor locations for the measurements of key operating parameters are shown in Fig. 3. Air temperature and humidity measurements were made by using HOBO data logger [2] at six locations near the top of cooling fan shroud. Water temperatures at the cell exit were also measured by waterproof Tidbit data logger at 0.7m above the free surface of collection basin. Water flow rate and temperature at the inlet of the distribution deck were measured by Doppler ultrasonic meter and Tidbit, respectively. Measurement data for each sensor location were recorded at a time interval of 15 minutes during six-month period in 2005. Test data for ambient air temperature and humidity including wind speed and directions at the inlet of the cell were continuously obtained from SRNL meteorology station. The data recorded by the sensor logger were downloaded to the computer, and they were averaged over 1-hour period for the benchmarking database to validate the model. The measurement conditions and test results for each test case are summarized in Table 1. Test results were used to benchmark and validate the model.

Model Validation

The analysis consists of two major parts. One part is to develop a model for the operation facility used to simulate counter-current flow MDCT to benchmark the calculations with and without cooling fan operations. The second part is to calculate the flow patterns for the turbulent flow induced by fan and wind and to investigate fan and wind effects on water cooling inside the cell when cooling fans are operated and they are turned off.

The modeling work considers three basic cases with different operating conditions to examine how sensitive the flow patterns are to different fan and wind speeds. The basic cases are fast fan and no fan as shown in Table 1. Flow patterns coupled with heat and mass transfer were calculated to evaluate the effect of water cooling inside the cell of the cooling tower. A three-dimensional CFD approach was used to solve the governing equations for the flow domain as shown in Fig. 1.

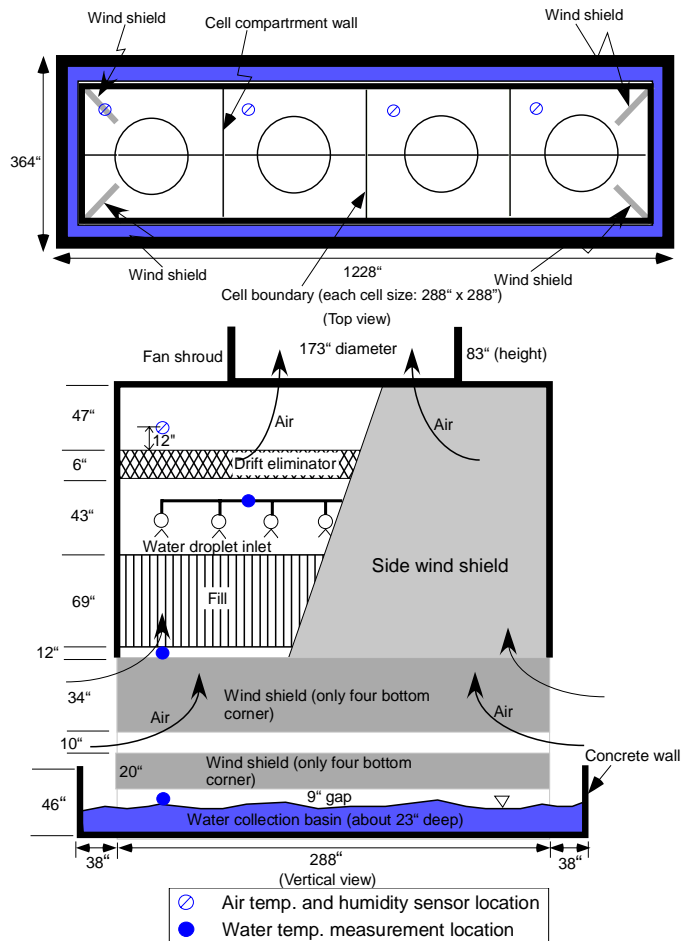


Fig. 3. Cross-section view of the compartment cell instrumented for the performance measurement.

Table 1. Test conditions and results

Test cases (2005)	Ambient conditions			T _{wi} (°C)	m _w kg/sec	T _{cell, exit} (°C), RH, (fan-on:1, fan-off:0)			
	T _{amb} (°C)	RH	U _o , θ _o			1 st cell	2 nd cell	3 rd cell	4 th cell
July21	24.40	0.86	0.71, 223	28.02	329.4	25.67, 0.99, (1)	25.56, 1.0, (1)	25.23, 1.0, (1)	28.02, 0.99, (1)
July22	25.17	0.80	0.81, 216	27.84	329.4	25.69, 0.98, (1)	25.56, 0.97, (1)	25.17, 0.96, (1)	25.17, 0.98, (1)
July26	28.22	0.68	1.0, 189	28.92	337.2	27.21, 0.98, (1)	26.73, 1.0, (1)	26.73, 1.0, (1)	26.73, 0.95, (1)
Aug8	27.44	0.77	1.25, 225	28.05	319.4	26.34, 0.97, (1)	26.34, 1.0, (1)	26.02, 1.0, (1)	26.03, 1.0, (1)
Aug14a	24.01	0.94	1.34, 169	26.15	316.1	24.40, 0.98, (1)	24.27, 0.97, (1)	24.08, 0.99, (1)	24.40, 0.99, (1)
Aug28	24.40	0.94	0.95, 56	27.56	449.2	25.95, 0.98, (1)	25.56, 0.99, (1)	25.46, 0.99, (1)	25.66, 1.0, (1)
Sep2	21.33	0.81	1.32, 344	22.72	416.8	21.71, 0.96, (1)	21.33, 0.95, (1)	21.14, 0.95, (1)	21.33, 0.95, (1)
Sep26a	21.33	0.98	2.04, 137	23.80	426.7	22.09, 1.0, (1)	22.09, 1.0, (1)	22.09, 1.0, (1)	22.09, 1.0, (1)
Sep28	27.12	0.70	4.06, 102	27.25	646.3	26.34, 0.97, (1)	25.76, 1.0, (1)	25.56, 1.0, (1)	25.95, 1.0, (1)
Sep29	19.60	0.97	0.63, 57	22.95	562.6	21.12, 1.0, (1)	21.16, 1.0, (1)	20.81, 1.0, (1)	21.02, 0.92, (1)
Sep29p	28.60	0.69	3.51, 278	25.46	635.1	25.13, 0.98, (1)	24.69, 1.0, (1)	24.98, 1.0, (1)	25.13, 0.97, (1)
Oct15	16.82	0.78	1.49, 179	18.22	369.3	16.95, 0.94, (0)	17.08, 0.95, (1)	16.63, 0.96, (1)	16.70, 0.95, (1)
Oct20	21.22	0.74	1.71, 188	22.62	380.7	21.49, 0.91, (0)	21.28, 0.91, (1)	21.11, 0.75, (0)	21.11, 0.87, (1)
Oct22	19.81	0.90	3.04, 274	24.19	391.3	22.09, 1.0, (0)	22.25, 1.0, (1)	22.25, 0.98, (0)	22.56, 1.0, (1)
Nov24	19.27	0.72	6.78, 268	24.65	477.1	23.24, 1.0, (0)	23.24, 1.0, (0)	23.24, 1.0, (0)	23.63, 1.0, (0)
Nov29	17.52	0.66	2.25, 231	20.62	511.6	19.33, 1.0, (1)	18.09, 1.0, (1)	20.19, 0.99, (0)	19.62, 1.0, (1)
Dec3	16.71	0.21	2.85, 160	22.07	442.1	22.31, 1.0, (0)	21.38, 1.0, (0)	21.60, 1.0, (0)	21.82, 1.0, (0)
Dec4	22.35	0.96	4.13, 197	24.04	549.0	23.57, 1.0, (0)	21.46, 1.0, (1)	22.80, 1.0, (0)	24.01, 1.0, (0)
Dec4m	20.19	1.0	2.43, 187	24.36	577.3	23.11, 1.0, (0)	21.58, 0.99, (1)	21.78, 0.97, (0)	21.46, 1.0, (0)
Dec5	17.67	1.0	2.80, 188	23.17	676.8	20.57, 1.0, (0)	19.89, 1.0, (1)	20.34, 1.0, (1)	18.96, 1.0, (0)

The modeling work considers three basic cases with different operating conditions to examine how sensitive the flow patterns are to different fan and wind speeds. The basic cases are fast fan and no fan as shown in Table 1. Flow patterns coupled with heat and mass transfer were calculated to evaluate the effect of water cooling inside the cell of the cooling tower. A three-dimensional CFD approach was used to solve the governing equations for the flow domain as shown in Fig. 1.

A prototypic geometry and domain of the cooling tower was created by a commercial finite volume code, FLUENT [3], and then it was meshed in non-orthogonal way to solve the governing equations. From the analysis of mesh sensitivity, about 3 million hexahedral meshes were established to perform the calculations. The finite volume method with the adoption of an iterative procedure based on the semi-implicit method of pressure-velocity coupling was used for the present study. The grid distribution was non-uniform with smaller mesh size for the cell regions of the cooling tower. The iterative solution is considered as converged when the normalized residual errors of all the independent variables solved are reduced at least by three orders and the average exit air temperature is changed less than 0.01°C. The values of other variables have also been monitored during the iteration to make sure the convergent solution of all the variables at the end of iteration process.

Drift eliminators inside the cells were modeled as porous media by using Ergun's equation [4]. About 77% porosity was estimated for the 0.15m thick drift region from the literature data [1].

The flow conditions for the cooling tower operations are assumed to be fully turbulent since Reynolds numbers for typical operating conditions are in the range of 10^6 . A standard two-equation turbulence model, referred to as $k-\epsilon$ model [5], was used since benchmarking results against the literature data showed that the model predicts turbulent flow evolution in a large fluid domain with reasonable accuracy [1,6]. Although other turbulent models such as RSM have the potential to give more accurate results for flows in which streamline curvature, swirl, rotation, or rapid changes near the wall boundary might be important, the standard $k-\epsilon$ model is considered a good model for the current calculations over a large fluid domain of mechanical drift cooling tower with fully-developed turbulent flow medium. The results demonstrate that the $k-\epsilon$ model combined with standard wall functions generally predicts the test results better than other models [7]. Its predictions agree with the data within about 15%.

The literature correlation [8] was used to calculate the heat and mass transfer from water droplets to the continuous gas phase at steady state, assuming them to be spherical and uniform. Based on the literature information [9] and computational efficiency, the model used the fixed droplet diameter to be 3 mm for the present analysis. As shown in Fig. 4, the present model was benchmarked against the test results available in the literature [10]. The calculation results show

that when single droplet is less than 4mm diameter, the model predicts the data by about 10% on the average. The experimental observations [10] clearly show that when droplet are larger than 4mm, it become non-spherical during free falling period. The integral benchmarking calculations for the counter-current cooling tower used the uniform droplet size of 3 mm diameter based on the experimental observation.

BENCHMARKING RESULTS AND DISCUSSIONS

Modeling predictions for turbulent airflow behavior and heat transfer characteristics were benchmarked against the literature data conducted under the simple geometrical systems. The verified model was extended to the prototypic MDCT system coupled with air humidification process to perform the integral benchmarking tests. The test cases for the SRS cooling tower consist of three basic cases.

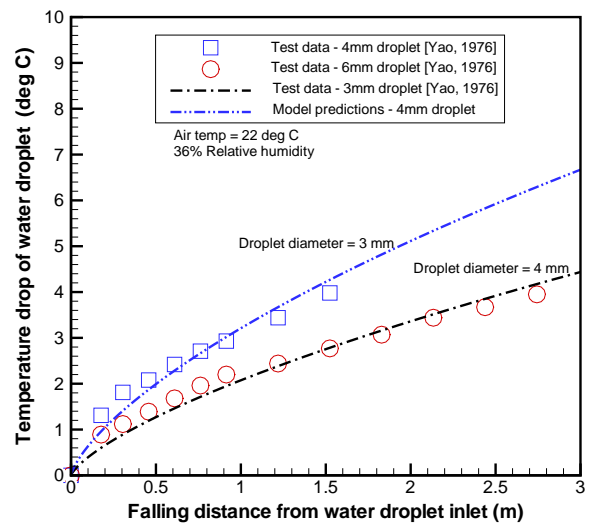


Fig. 4. Comparison of the predicted droplet cooling with the test data for free-falling water droplet in still air [10].

As shown in Table 1, they are typically two different air velocities at shroud exit, depending on the fan speeds of the cooling tower. They are normal fan speed with about 10 m/sec air speed and fan-off case with no forced convection. Average computational time for each of the test cases was about 4 days using two-cpu parallel run under HP DL585 Linux IBM workstation.

The modeling predictions for air velocity around the cooling tower under the different operating conditions are compared with the SRNL test results as shown in Table 1. The results show that the predictions reasonably agree with the test data. Fig. 5 shows air flow patterns for the vertical mid-plane

crossing the 3rd cell of the cooling tower for low wind speed of less than 1 m/sec under the operating conditions of the Aug28 case. As shown in the figure, it is noted that there is negligible impact of wind speed on air flow patterns at the shroud exit. The corresponding air temperature and humidity at the shroud exit are shown in Figs. 6 and 7. Water droplet temperatures were calculated along the trajectory within each cell via Lagrangian approach, assuming droplet size to be uniform and 3 mm diameter. The temperature distributions for water droplet under the Aug28 case are shown in Fig. 8.

Figure 9 compares the vapor contents inside air between the fan-on and fan-off cells when two cooling fans of the 1st and 4th cells are turned off under the cool and humid ambient conditions of the Dec5 case. The modeling results show that when wind speed gets higher, air temperature inside the fan-off cell is distributed in more asymmetrical way across the upstream and downstream sides because heat transfer performance from water droplet to air becomes better with air speed increased. These are consistent with the literature results [8]. Table 2 compares the results for vapor mass fractions at cell exit air for various ambient conditions under partially or totally fan-off cells. As shown in the table, it is noted that when less humid air is introduced into the fan-off cell with high wind speed, it is humidified by the falling water with about the same level as that of the fan-on cell.

Figure 10 compares the predictions with measured air temperatures at the cell exit of the H-area cooling tower. The corresponding vapor contents contained in the air are compared in Fig. 11. The results show that the model can predict the air temperature and humidity within about 15%. It is demonstrated that the CFD model for the counter-current MDCT system captures basic flow patterns and heat transfer characteristics, and it predicts the test results in a reasonably accurate way.

Based on the benchmarked model, calculations for the cell exit velocities were performed for various wind speeds and directions under the counter-current MDCT system at SRS. Figure 12 shows the results for three different wind speeds as function of wind direction under fan-off conditions when cell exit velocity and wind direction are nondimensionalized by wind speed and 180°, respectively. The results show that when wind approaches toward the narrower side of the tower, cell exit velocity is at minimum due to the wind shield effect as shown in Fig. 3. It is also noted that as wind speed increases, air velocity at cell exit increases a little bit for the Bernoulli effect due to the presence of the flow obstructions.

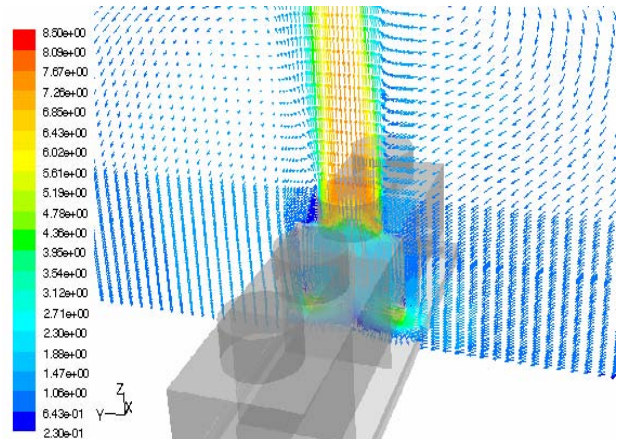


Fig. 5. Air flow patterns for the vertical mid-plane crossing the 3rd cell of the cooling tower for low-speed wind in H-Area cooling tower (Aug28 case).

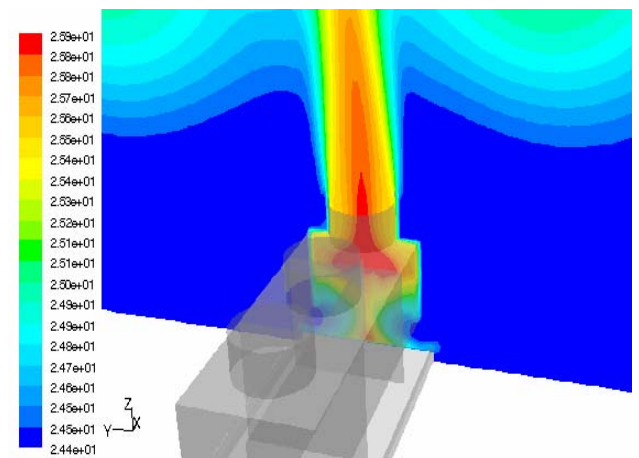


Fig. 6. Air temperature distributions for the vertical mid-plane crossing the 3rd cell of the cooling tower for low-speed wind in H-Area cooling tower (Aug28 case), showing that red-color zone indicates about 26°C.

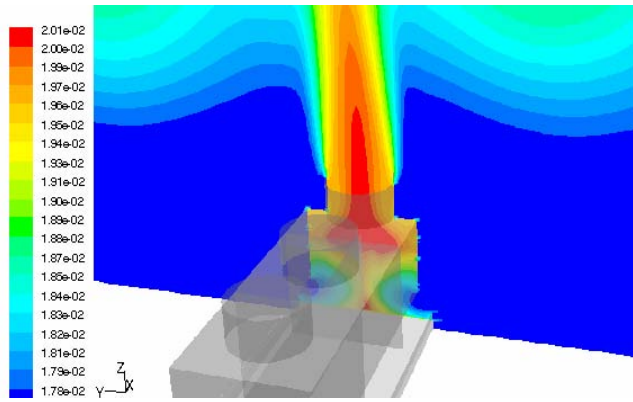
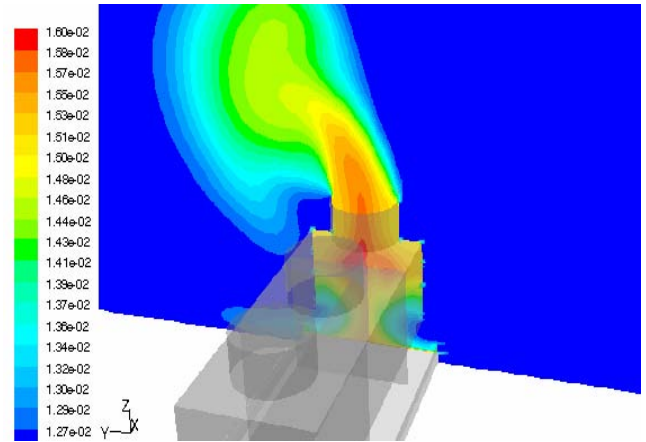


Fig. 7. Vapor mass fractions for the vertical mid-plane crossing the 3rd cell of the cooling tower for low-speed wind in H-Area cooling tower (Aug28 case), showing that red-color zone indicates about 2.0% mass fraction.



(Dec5 case: fan-on cell)

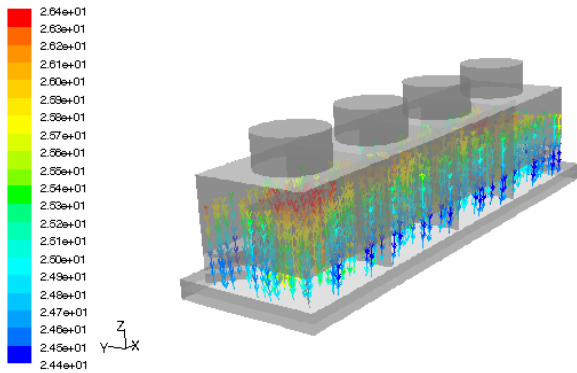
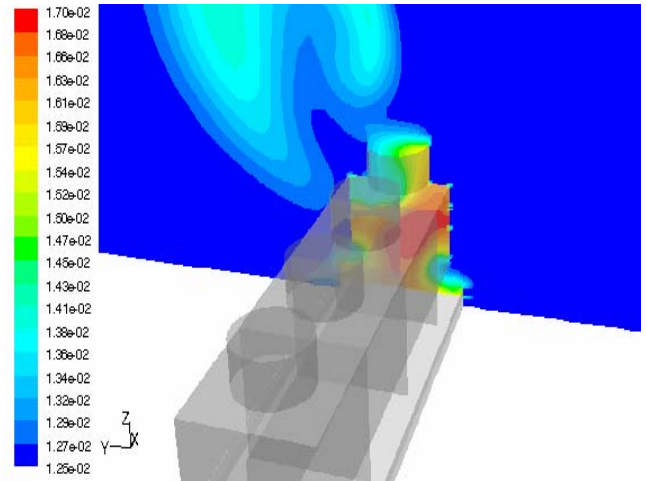


Fig. 8. Temperature distributions for water droplets for the Aug28 case



(Dec5 case: fan-off cell)

Fig. 9. Comparison of air mass fraction distributions between fan-on and fan-off cells at the plane crossing the vertical center of the cell

Table 2. Results for vapor mass fractions at cell exit for various ambient conditions under partially or totally fan-off cases

Cases	Ambient conditions			Averaged vapor mass fraction at cell exit (γ_{exit})			
	T_{amb}	γ_{amb}	U_o	Fan-off cell		Fan-on cell	
				Data	Pred.	Data	Pred.
Oct15	16.82	0.0092	1.49	0.0112	0.0102	0.0113	0.0112
Oct20	21.22	0.0115	1.71	0.0144	0.0136	0.0131	0.0130
Oct22	19.81	0.0129	3.04	0.0165	0.0178	0.0168	0.0167
Nov24	19.27	0.0100	6.78	0.0181	0.0180	--	--
Dec3	16.71	0.0025	2.85	0.0162	0.0151	--	--
Dec4	22.35	0.0161	4.13	0.0179	0.0177	0.0159	0.0177
Dec4m	20.19	0.0147	2.43	0.0164	0.0160	0.0158	0.0177
Dec5	17.67	0.0125	2.80	0.0143	0.0146	0.0146	0.0155

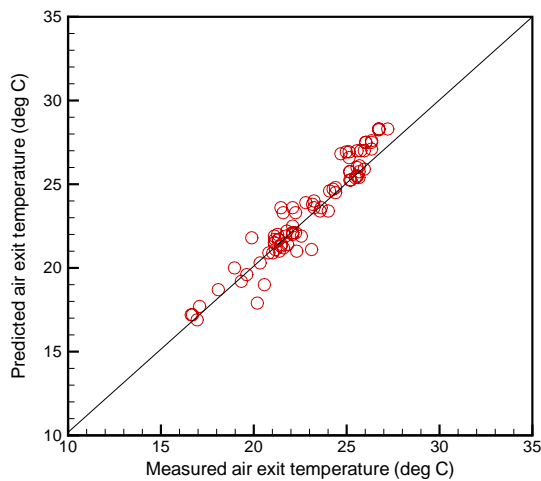


Fig. 10. Comparison of the model predictions with the test results for air exit temperature.

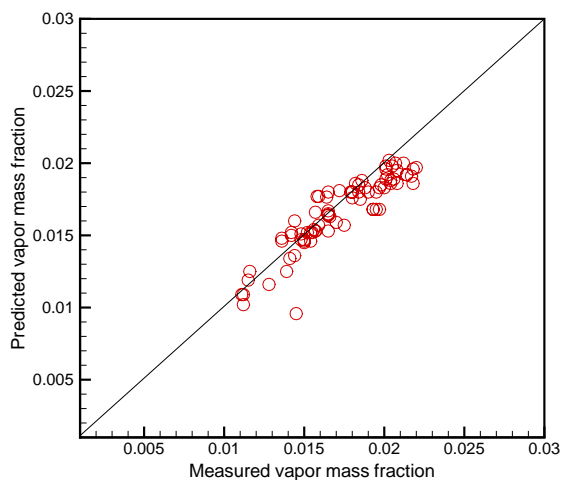


Fig. 11. Comparison of the model predictions with test results for vapor mass fractions at shroud exit.

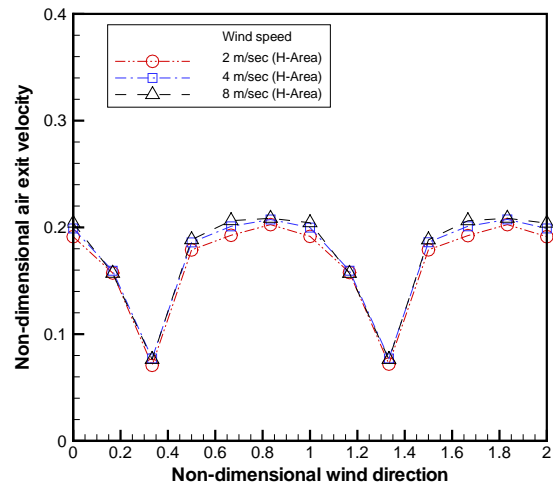
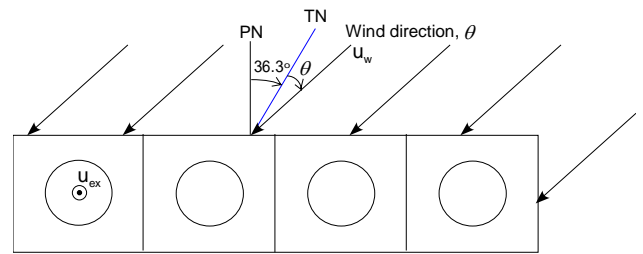


Fig. 12. Nondimensional air velocities at shroud exit as function of wind direction for three different wind speeds under fan-off conditions

CONCLUSION

A three-dimensional steady-state CFD model was developed for the SRS four-cell MDCT system to evaluate the flow patterns and heat transfer characteristics inside the cooling cell driven by cooling fan and wind. It used standard two-equation turbulence model to capture turbulent flow behavior of air inside and outside the tower cells. The model considers the air-vapor mixture coupled with water droplet component, assuming that vapor phase is always transported by the continuous air phase with no slip velocity. In this work, water droplet component was considered as discrete phase via Lagrangian approach for the evaporative heat transfer. Experiments were conducted to obtain the benchmarking database for verifying the CFD model.

A series of the modeling calculations was performed to investigate the impact of the ambient and operating conditions on flow patterns and heat transfer characteristics inside the cell of the counter-current cooling tower. The modeling predictions are in reasonably good agreement with the test results. It is also demonstrated that CFD method is applicable to the detailed modeling analysis for the large-scaled cooling tower system.

ACKNOWLEDGMENT

This work was funded by U.S. Department of Energy and performed at the Savannah River National Laboratory, which is operated by the Savannah River Nuclear Solutions, LLC.

REFERENCES

- [1] S. Y. Lee, A. J. Garrett, J. S. Bollinger, and L. D. Koffman, "CFD Modeling Analysis for Mechanical Draft Cooling Tower", 2008, ASME 2008 Summer Heat Transfer Conference, HT-2008-56080, Jacksonville, Florida.
- [2] HOBO Water Temp Pro Logger, www.microdaq.com.
- [3] FLUENT, 2006, Fluent, Inc., Lebanon, New Hampshire.
- [4] S. Ergun, 1952, "Fluid through Packed Columns", *Chemical Engineering Progress*, Vol. 18, No. 2, pp. 87.
- [5] W. P. Jones and P. E. Launder, 1972, "The Prediction of Laminarization with a Two-Equation Model of Turbulence", *Int. Journal of Heat and Mass Transfer*, Vol. 15, pp. 301-314, 1972.
- [6] P. V. Nielsen, A. Restivo, and J. H. Whitelaw, 1978, "The Velocity Characteristics of Ventilated Rooms", *ASME J. of Fluids Engineering*, Vol. 100, pp. 291-298.
- [7] S. Y. Lee, R. A. Dimenna, R. A. Leishear, D. B. Stefanko, 2008, "Analysis of Turbulent Mixing Jets in a Large Scale Tank", *ASME Journal of Fluids Engineering*, Volume 130, Number 1, pp. 011104.
- [8] W. E. Ranz and W. R. Marshall, Jr., 1952, Part II, "Evaporation from Drops", *Chemical Eng. Progress*, vol. 48, pp. 173-180.
- [9] S. P. Fisenko, A. A. Brin, and A. I. Petrushik, 2004, "Evaporative Cooling of Water in a Mechanical Draft Cooling Tower", *Int. J. of Heat and Mass Transfer*, Vol. 47, pp. 165-177.
- [10] S. C. Yao and V. E. Schrock, 1976, "Heat and Mass transfer from Freely Falling Drops", *Trans. ASME J. of Heat Transfer*, pp. 120-126.